



# Co-rich Amorphous Microwires with Improved Giant Magnetoimpedance Characteristics Due to Glass Coating Etching

V.A. BAUTIN <sup>1,3</sup>, N.S. KHOLODKOV,<sup>1</sup> A.V. POPOVA,<sup>2</sup>  
S.A. GUDOSHNIKOV,<sup>1,2</sup> and N.A. USOV<sup>1,2</sup>

1.—National University of Science and Technology «MISiS», Moscow, Russia 119049. 2.—Pushkov Institute of Terrestrial Magnetism, Ionosphere and Radio Wave Propagation, Russian Academy of Sciences, (IZMIRAN), Troitsk, Moscow, Russia 108480. 3.—e-mail: bautin@list.ru

Glass-coated Co-rich amorphous microwires are very promising for the development of tiny magnetic sensors that can be used in portable electronic devices. In this study, a substantial decrease in the residual quenching stress in Co-rich microwires is achieved by reducing the thickness of the glass coating by means of precise etching of the wire in a specially designed gel. This effect is confirmed experimentally by means of the small-angle magnetization rotation method as well as by direct measurement of the off-diagonal component of the giant magnetoimpedance (GMI) tensor of wires with different thicknesses of glass coating as a function of the applied magnetic field. A reduction in the thickness of the glass coating to the range of 0.5–2.0  $\mu\text{m}$  resulted in a nearly twofold increase in the steepness of the off-diagonal GMI component of the studied Co-rich microwires. Therefore, this method can be used to improve the sensitivity of miniature magnetic sensors to weak external magnetic fields.

## INTRODUCTION

Due to the rapid development of telecommunication and data transmission systems, much attention is now being paid to control of environmental electromagnetic radiation to ensure human safety and robust operation of critical equipment. To achieve continuous monitoring of the surrounding electromagnetic field, portable electronic devices can be equipped with miniature sensors that can detect weak magnetic fields. The sensing element of such magnetic sensors may be a small section of glass-coated amorphous ferromagnetic microwire (AFM) with total diameter of 10  $\mu\text{m}$  to 30  $\mu\text{m}$ .<sup>1–6</sup>

The main advantage of such sensors based on the giant magnetoimpedance (GMI) effect in Co-rich amorphous microwire with negative magnetostriction<sup>4–6</sup> is their small size and low weight, as well as very high sensitivity to weak magnetic fields. These parameters play a crucial role for portable devices. In addition, such AFM sensors are relatively inexpensive. Moreover, suitable postproduction treatments of Co-rich amorphous microwires can further

improve their magnetic and GMI characteristics.<sup>1,2,7</sup> Thermal treatment of AFM can be achieved by Joule heating by passing a direct current (DC) or alternating current (AC) along the microwire or by conventional furnace annealing.<sup>7–12</sup> Joule heating using a DC or AC current can also be performed in a longitudinally applied magnetic field of about several kA/m, as well as under the influence of applied tensile or torsion stresses.<sup>7,13,14</sup>

It is generally accepted<sup>15–20</sup> that the magnetic characteristics of AFM are mainly determined by the distribution of the significant residual quenching stress over the microwire cross-section. This residual stress arises during the formation of the wire from the melt, mostly due to the difference in the linear expansion coefficients of the inner ferromagnetic core and outer glass shell. Other origins of residual stress include quenching stresses produced by rapid quenching of the metallic alloy from the melt, as well as axial stresses related to wire drawing.<sup>15</sup> A properly chosen annealing procedure can significantly reduce the magnitude of the residual quenching stress in amorphous microwires. For

Co-rich amorphous microwires with negative magnetostriction, this can lead to a decrease in the wire anisotropy field and thus an increase in the magnetic permeability and GMI ratio.<sup>1,2,7,14</sup>

On the other hand, it is well known<sup>15–18</sup> that the magnitude of the residual quenching stress in an amorphous glass-coated microwire depends on its geometrical characteristics, i.e., the diameter of the ferromagnetic core  $d$  and the total wire diameter  $D$ , as well as the ratio  $\rho = d/D$ . It has been demonstrated experimentally<sup>7,21–23</sup> that the magnetic permeability and GMI ratio of Co-rich amorphous microwires with negative magnetostriction constant usually increase as a function of  $\rho$ ; i.e., for microwires with relatively small glass coating thickness,  $t_{sh} = (D - d)/2$ . Therefore, decreasing the thickness of the glass coating using etching or other methods has long been recognized<sup>24–29</sup> as a promising method to decrease the magnitude of the residual quenching stress and improve the magnetic softness of Co-rich amorphous microwires with negative magnetostriction constant. However, in this approach, it is important to ensure precise control of the final thickness of the glass coating and achieve low roughness of the glass surface after etching.

Recently, it was shown<sup>30</sup> that the magnitude of the residual quenching stress can be considerably diminished by precise etching of the glass coating on the wire in a specially designed gel. Using the method of small-angle magnetization rotation,<sup>31–33</sup> it was proved<sup>30</sup> that, at the initial stage of etching, the magnitude of the residual quenching stress decreases on average by 40% to 50% per micrometer reduction of the glass coating thickness.

Based on physical considerations, it is clear that a decrease in the magnitude of the residual quenching stress should lead to a reduction of the anisotropy field of the microwire and thus an increase of its GMI characteristics in weak longitudinal magnetic fields.<sup>7,19,29</sup> In the work presented herein, this effect is confirmed experimentally by direct measurement of the off-diagonal component of the GMI tensor of wires with different thicknesses of glass coating as a function of the applied magnetic field. It is found that a reduction in the glass coating thickness by  $0.5 \mu\text{m}$  to  $1.0 \mu\text{m}$  leads to an increase in the steepness of the off-diagonal GMI component by 30% to 40%. This effect could be used to achieve a notable increase in the sensitivity of AFM magnetic sensors.

## EXPERIMENTAL PROCEDURES

Co-rich AFMs consisting of a ferromagnetic core with composition  $\text{Co}_{71}\text{Fe}_4\text{Si}_{10}\text{B}_{15}$  in a glass shell were fabricated by the Taylor–Ulitsky method.<sup>1,2,29,30</sup> The microwires were wound using a coil with diameter of 0.05 m. For etching of the glass coating, four segments of microwire with length from 0.14 m to 0.155 m, roughly

corresponding to the circumference of the coil, were cut. The geometric dimensions of the samples and the parameters of the wire production process are presented in Table I, where  $W$  is the winding speed and  $V_{gl}$  is the feed rate of the glass tube. As an example, Fig. 1a shows the open ferromagnetic core of sample 1, whereas Fig. 1b shows a general view of the same sample with the glass shell.

Table I reveals that samples 1 to 4, cut from the same piece of microwire obtained using standard Taylor–Ulitsky equipment, exhibited small long-range variations in both the diameter of the ferromagnetic core and the thickness of the glass coating. Nevertheless, proper posttreatment can help improve the GMI characteristics of these samples to make them suitable for use in sensor applications.

## Precision Etching of Wire Coating

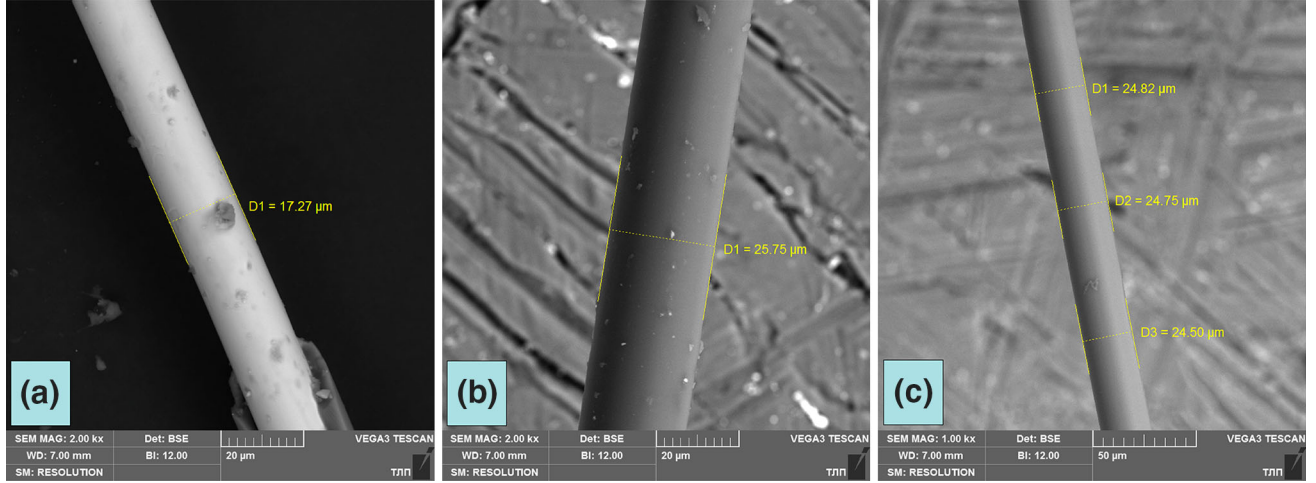
Mechanical removal is occasionally used to scrape the glass coating off the microwire completely. However, this operation can lead to damage of the amorphous ferromagnetic core and does not allow investigation of the change in the AFM characteristics depending on the thickness of the glass coating. Precision etching of the glass coating on the microwire in a specially designed gel<sup>30</sup> enables one to change the thickness of the glass coating on the wire with high precision. In addition, this technique makes it possible to obtain a glass surface with small finite roughness. Note that solutions used for glass etching based on HF acid<sup>34,35</sup> have high toxicity and result in an etched glass surface with roughness of no less than 600 nm.

The special gel used for etching the glass coating contained the following components by weight percent:<sup>30</sup> propylene glycol (60.3% to 60.9%), ammonium fluoride acid (7.27% to 7.88%), ethyl alcohol (4.24% to 4.85%), and sucrose (2.12% to 2.73%). The other components were water and special surface-active additives. First, solution 1 was prepared by grinding 0.025 kg ammonium fluoride acid and dissolving it in  $66 \times 10^{-6} \text{ m}^3$  water at temperature of 25°C. To prepare solution 2, 0.008 kg sucrose was dissolved in  $16 \times 10^{-6} \text{ m}^3$  water and  $15 \times 10^{-6} \text{ m}^3$  ethyl alcohol was added, followed by addition of  $201 \times 10^{-6} \text{ m}^3$  propylene glycol, previously heated in a water bath to 50°C to 60°C. Then, solution 2 was cooled to 25°C. The final step was to mix solution 1 and solution 2 and add surfactant.

Due to its reduced concentration of active fluoride ions, this etching gel has low toxicity and achieves high etching uniformity. Due to hydrolysis, ammonium fluoride acid results in formation of hydrofluoric acid, which dissolves the glass coating of the microwire. Use of this gel enables etching of the glass coating at a rate of  $0.23 \mu\text{m/h}$  to  $1.96 \mu\text{m/h}$  with a surface roughness from 40 nm to 100 nm, depending on the etching depth.

**Table I. Composition and parameters of Co-rich microwires**

No.	$d$ ( $\mu\text{m}$ )	$D$ ( $\mu\text{m}$ )	$t_{\text{sh}}$ ( $\mu\text{m}$ )	Composition	$W$ (m/min)	$V_{\text{gl}}$ (mm/min)
1	17.27	25.75	4.24	$\text{Co}_{71}\text{Fe}_4\text{Si}_{10}\text{B}_{15}$	140	1.8
2	17.26	25.29	4.02			
3	18	27.51	4.76			
4	17.89	27.21	4.66			


 Fig. 1. (a) Released ferromagnetic core of sample 1 with diameter  $d = 17.27 \mu\text{m}$ ; (b) glass coating of the wire before etching ( $D = 25.75 \mu\text{m}$ ); (c) glass coating after etching with average diameter ( $D$ ) =  $24.69 \mu\text{m}$ .

It was found recently<sup>30</sup> that a significant drop in the magnitude of the residual quenching stress occurs after removal of the initial coating layers with thickness on the order of  $1 \mu\text{m}$ . In the prepared gel, this occurs during the first 20 min to 30 min of the etching process. As an example, Fig. 1b and c shows the initial and final glass coating surface of sample 1 immersed in gel for 20 min. It is worth noting in Fig. 1c the very small fluctuations of the outer diameter of the glass coating obtained after etching in the gel.

### Residual Quenching Stress

A modified small-angle magnetization rotation method<sup>31,32</sup> was used to measure the magnitude of the residual quenching stress in AFMs with different thicknesses of glass coating. In this method, a long piece of Co-rich AFM is placed in an applied magnetic field  $H_{0z}$ , which is sufficiently large in comparison with the effective anisotropy field of the wire,  $H_{a,\text{ef}} = 2K_{\text{ef}}/M_s$ , where  $M_s$  is the saturation magnetization of the wire,  $K_{\text{ef}} = 3|\lambda_s|(\Delta\sigma + \sigma_{zz}^{(a)})/2$  is the effective magnetic anisotropy constant,  $\lambda_s$  is the magnetostriction constant,  $\Delta\sigma$  is the magnitude of the residual quenching stress, and  $\sigma_{zz}^{(a)}$  is the tensile mechanical stress applied to the wire.

In a sufficiently strong longitudinal magnetic field,  $H_{0z} \gg H_{a,\text{ef}}$ , the magnetic moment of the wire

is almost parallel to its axis, so the circular component of the unit magnetization vector is close to zero. Consider an alternating current with frequency  $f$  and amplitude  $I_0$ ,  $I(t) = I_0 \sin(\omega t)$ , where  $\omega = 2\pi f$  is the angular frequency, flowing through the microwire. Under the influence of the circular magnetic field of the alternating current, the circular component of the unit magnetization vector experiences small oscillations with frequency  $\omega$ . This generates an electromotive force  $E$  at twice the frequency in a small receiving coil wound on the amorphous microwire:

$$E = E_{2f}(H_{0z}) \sin(2\omega t). \quad (1)$$

The amplitude of the second harmonic of the electromotive force is given by the equation<sup>32</sup>

$$E_{2f}(H_{0z}) = \frac{C_{2f}}{(H_{a,\text{ef}} - H_{0z})^2}; C_{2f} = \frac{4\pi^2 M_s N \omega I_0^2}{c^3}, \quad (2)$$

where  $c$  is the speed of light and  $N$  is the number of turns in the receiving coil.

In this work, the amplitude of the second harmonic of the electromotive force was measured in the range of the external magnetic field  $H_{0z}$  from 0 mT to 2 mT, with an amplitude of the alternating current of  $I_0 = 10 \text{ mA}$ , and with various tensile stresses applied to the wire by attaching small masses of  $0.4 \times 10^{-3} \text{ kg}$  to  $4.4 \times 10^{-3} \text{ kg}$  to the

lower end of the vertically suspended wire. The frequency of the alternating current was  $f = 5$  kHz, and the number of turns of the receiving coil was  $N = 200$ .

For sample 1, with an initial ratio of internal and external diameters of  $d/D = 0.671$  and an initial thickness of the glass coating of  $t_{\text{sh}} = 4.24 \mu\text{m}$ , the magnetostriction constant was determined to be  $\lambda_s = -2.9 \times 10^{-7}$ , the saturation magnetization of the wire being  $M_s = 500 \pm 10$  kA/m. The reduced magnitude of the residual quenching stress in this wire before etching was found to be  $\Delta\sigma/\sigma_0 = 1.8$ , where  $\sigma_0 = 100$  MPa is the characteristic magnitude of the residual quenching stress.

After etching sample 1 in the gel for 20 min, the thickness of the glass coating decreased to  $t_{\text{sh}} = 3.71 \mu\text{m}$ . As a result, the reduced magnitude of the residual quenching stress diminished to  $\Delta\sigma/\sigma_0 = 0.25$ . Other parameters of the wire, such as the magnetostriction constant and the saturation magnetization, remained unchanged, since etching the glass coating does not affect the ferromagnetic core of the microwire. Similar changes of the residual quenching stress due to etching were obtained also for samples 2 to 4, as shown in Table I.

### GMI Characteristics

Measurements of the off-diagonal component of the GMI tensor were carried out for the samples presented in Table I before and after etching of the glass coating. By definition,<sup>36</sup> the off-diagonal component of the GMI tensor is given by  $Z_{\varphi z}(H_{0z}) = e_{\varphi}(R)/I_z$ , where  $e_{\varphi}(R)$  is the value of the circular component of the electric field,  $e_{\varphi}(R)$ , on the wire surface,  $r = R$ , and  $I_z$  is the amplitude of the alternating current flowing through the microwire. Due to the small diameter of the microwire, it is convenient, however, to measure the circular component of the electric field at some distance  $R_c$  from the wire center. This can be done<sup>37</sup> by measuring the magnitude of the electromotive force,  $E = 2\pi R_c N_c e_{\varphi}(R_c)$ , that occurs in a thin receiving coil of radius  $R_c$  wound around the wire, where  $N_c$  is the number of turns of the receiving coil.

Note that the amplitude of the circular component of the electric field outside the wire,  $r \geq R$ , is determined by the equation<sup>36</sup>

$$e_{\varphi}(r) = D \frac{ik_0}{p} H_1^{(2)}(pr), \quad (3)$$

where  $D$  is the amplitude coefficient,  $p = \sqrt{k_0^2 - \beta^2}$ ,  $\beta$  is the longitudinal wavenumber,  $k_0 = \omega/c$ , and  $H_1^{(2)}(x)$  is Hankel's function.<sup>38</sup> Therefore, the ratio between the circular electric component on the wire surface,  $r = R$ , and at some distance  $r = R_c$  from the wire center is given by

$$\frac{e_{\varphi}(R_c)}{e_{\varphi}(R)} = \frac{H_1^{(2)}(pR_c)}{H_1^{(2)}(pR)} \approx \frac{R}{R_c}. \quad (4)$$

Actually, it can be shown that, due to the small values of the radii  $R$  and  $R_c$ , the arguments of the Hankel's functions are also small at modest frequencies ( $pR, pR_c \ll 1$ ). Therefore, in Eq. 4, one can use the asymptotic result for Hankel's function at small arguments:<sup>38</sup>  $H_1^{(2)}(x) \approx 2i/\pi x$ , yielding  $Z_{\varphi z}(H_{0z}) = R_c e_{\varphi}(R_c)/RI_z$ .

The experimental setup to measure the GMI tensor component consisted of a magnetic field sweep source, a sinusoidal signal source with frequency  $f$  of 1 MHz to 10 MHz, a direct-current bias source, the measuring channel for recording the off-diagonal GMI tensor component, and a multi-purpose fast Fourier transform (FFT) signal analyzer CF-5210. In the present experiment, a receiving coil with internal radius of  $R_c = 0.5$  mm and  $N_c = 85$  turns of copper wire with diameter of  $50 \mu\text{m}$  was used.

A sample of microwire with length of  $\sim 0.01$  m was fixed inside the receiving coil, and its ends were soldered to the contact pads of a special holder. The holder was connected to the measuring system using 0.5-m-long shielded twisted pairs and was located inside the Helmholtz coil system placed in a Permalloy magnetic shield. During the measurements, a linearly varying magnetic field in the range of  $\pm 1.5$  mT can be created using the Helmholtz coils. A direct bias current in the range of  $\pm 5$  mA can also be passed through the microwire. The high-frequency signal of the off-diagonal GMI tensor component was amplified and then detected by a special device. The measured value of the off-diagonal GMI tensor component was normalized to the resistance of the wire at constant current,  $R_{\text{dc}} = \rho/\pi R^2$ , where  $\rho = 1.2 \times 10^{-6} \Omega/\text{m}$  is the specific resistance of the wire.

The symbols in Fig. 2 show the experimental data for the reduced off-diagonal component of the GMI

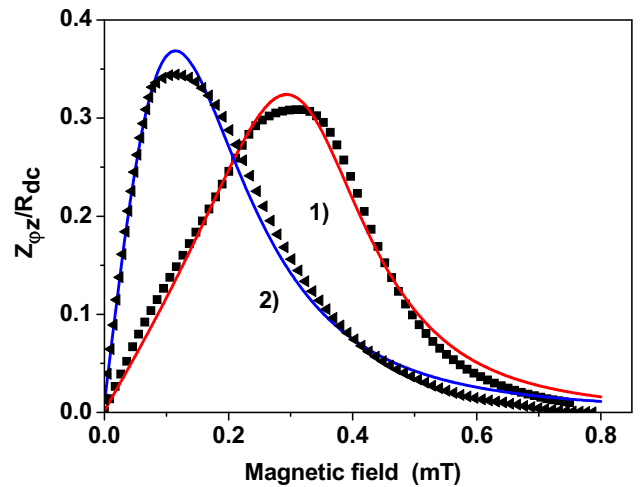


Fig. 2. Off-diagonal component of GMI tensor in sample 1 with various glass coating thicknesses: (1) initial microwire with  $t_{\text{sh}} = 4.24 \mu\text{m}$ , and (2) the same wire after etching with  $t_{\text{sh}} = 3.71 \mu\text{m}$ . Symbols are experimental data; solid curves are drawn according to theory<sup>37</sup>.



tensor for sample 1 at an alternating current frequency of  $f = 5$  MHz. The constant bias current was  $I_{dc} = 2$  mA, while the external longitudinal magnetic field was varied in the range of  $\pm 1$  mT. One can see that the dependence of the off-diagonal GMI component on the longitudinal magnetic field is much steeper for the wire with decreased thickness of the glass coating. The linear part of this characteristic in the range  $\pm 0.07$  mT can be used in the AFM sensor to measure the longitudinal component of a weak applied magnetic field.

It is physically obvious that the improvement in the GMI characteristics of the AFM is associated with a drop in the amplitude of the residual quenching stress due to the etching of the glass coating. The change in the magnitude of the residual quenching stress can also be estimated by theoretical calculation<sup>37</sup> of the off-diagonal component of the GMI tensor. To calculate this component, we use the saturation magnetization and magnetostriction constant of the amorphous wire determined above by means of the small-angle magnetization rotation method. The fitting parameters in the theory are the dimensionless magnetic damping constant, which in agreement with previous studies<sup>6,37</sup> is taken to be  $\kappa = 0.8$  to  $1.0$ , and the reduced magnitude of the residual quenching stress  $\Delta\sigma/\sigma_0$ .

Figure 2 shows a comparison of the experimental and theoretical data for the reduced off-diagonal component of the GMI tensor for sample 1, before and after etching the glass coating. The symbols in Fig. 2 correspond to the experimental data. The solid curves were calculated for the ratios  $\Delta\sigma/\sigma_0 = 1.7$  and  $\Delta\sigma/\sigma_0 = 0.25$  for the initial wire, and the wire with the reduced glass coating thickness, respectively. One can see from Fig. 2 that the steepness of the off-diagonal GMI component of the microwire,  $\Delta Z_{\varphi z}/R_{dc}\Delta H$ , increases from  $\sim 1.0$  1/mT up to  $\sim 2.8$  1/mT after etching the microwire.

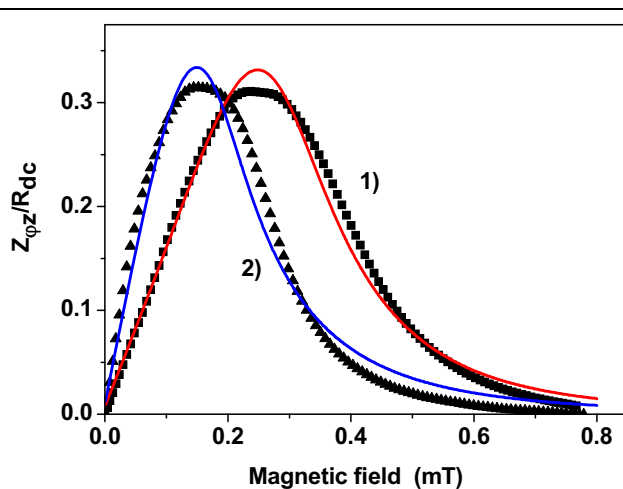


Fig. 3. Off-diagonal component of GMI tensor in sample 4 with various glass coating thicknesses: (1) initial microwire with  $t_{sh} = 4.66$   $\mu\text{m}$ , and (2) the same wire after etching with  $t_{sh} = 2.61$   $\mu\text{m}$ .

Similar results were also obtained for samples 2 to 4 in Table I. The off-diagonal component of the GMI tensor for sample 4 is shown in Fig. 3, where symbols represent the experimental data, while solid curves are drawn according to theory.<sup>37</sup> The etching of the glass coating for this microwire was carried out for 80 min. As a result, the thickness of the glass coating on the microwire decreased to  $t_{sh} = 2.61$   $\mu\text{m}$ . The magnetostriction constant for this microwire was determined to be  $\lambda_s = -3.5 \times 10^{-7}$ , the saturation magnetization being nearly the same as for sample 1.

Using the small-angle magnetization rotation method, the reduced magnitude of the residual quenching stress in this wire before etching was found to be  $\Delta\sigma/\sigma_0 = 1.5$ . After etching, it diminished to  $\Delta\sigma/\sigma_0 = 0.45$ . As a result, the steepness of the off-diagonal GMI component of the microwire,  $\Delta Z_{\varphi z}/R_{dc}\Delta H$ , increased from  $\sim 1.0$  1/mT to  $\sim 2.0$  1/mT.

Figures 2 and 3 clearly show reasonable agreement between the theoretical and experimental data for the off-diagonal component of the GMI tensor for both the original samples and those with reduced glass coating thickness. However, further experiments seem necessary to estimate the optimal reduction of the glass coating thickness for the Co-rich microwires studied.

## CONCLUSION

It is well known<sup>1,7-14,29</sup> that various types of thermal treatment can significantly improve the magnetic softness and GMI characteristics of Co-rich amorphous microwires, which is very promising for the development of miniature AFM magnetic sensors. In this paper, another promising technology is suggested for postproduction treatment of pieces of Co-rich microwire, viz. precise etching of the glass wire coating in a specially designed gel. The method produces a very smooth glass surface with roughness of 40 nm to 100 nm, depending on the etching depth. Direct measurements reveal that such reduction of the thickness of the glass coating on the microwire by means of precise etching leads to a significant increase in the steepness of the off-diagonal component of the GMI tensor of the wire. This is a consequence of a decrease in the magnitude of the residual quenching stress in the Co-rich microwire due to the etching. The steepness of the off-diagonal GMI component is found to increase nearly twofold after a reduction in the glass coating thickness by 0.5  $\mu\text{m}$  to 2.0  $\mu\text{m}$ . This makes the developed technology applicable to achieve a noticeable increase in the sensitivity of miniature AFM magnetic sensors for use in portable electronic devices.

## ACKNOWLEDGEMENT

The authors wish to acknowledge financial support from the Ministry of Education and Science of

the Russian Federation in the framework of the Increase Competitiveness Program of NUST «MISIS» (Contract No. K2-2017-008).

## REFERENCES

1. A. Zhukov and V. Zhukova, *Magnetic Properties and Applications of Ferromagnetic Microwires with Amorphous and Nanocrystalline Structure* (New York: Nova Science, 2009).
2. M.H. Phan and H.X. Peng, *Prog. Mater. Sci.* 53, 323 (2008).
3. H.X. Peng, P.F. Qin, and M.-H. Phan, *Ferromagnetic Microwire Composites: from Sensors to Microwave Applications* (Berlin: Springer, 2016).
4. K. Mohri and Y. Honkura, *Sens. Lett.* 5, 267 (2007).
5. V. Zhukova, M. Ipatov, and A. Zhukov, *Sensors* 9, 9216 (2009).
6. S. Gudoshnikov, N. Usov, A. Nozdrin, M. Ipatov, A. Zhukov, and V. Zhukova, *Phys. Status Solidi A* 211, 980 (2014).
7. A. Zhukov, V. Zhukova, J.M. Blanco, and J. Gonzalez, *J. Magn. Magn. Mater.* 294, 165 (2005).
8. V. Zhukova, A.F. Cobeno, A. Zhukov, J.M. Blanco, S. Puerta, J. Gonzalez, and M. Vazquez, *J. Non-Cryst. Solids* 287, 31 (2001).
9. L. Brunetti, P. Tiberto, F. Vinai, and H. Chiriac, *Mater. Sci. Eng. A* 304–306, 961 (2001).
10. A. Zhukov, A. Talaat, J.M. Blanco, M. Ipatov, and V. Zhukova, *J. Electron. Mater.* 43, 4532 (2014).
11. K.R. Pirota, L. Kraus, H. Chiriac, and M. Knobel, *J. Magn. Magn. Mater.* 226–230, 730 (2001).
12. M.H. Phan, Y.S. Kim, N.X. Chien, S.C. Yu, H.B. Lee, and N. Chau, *Jpn. J. Appl. Phys.* 42, 5571 (2003).
13. A. Zhukov, A. Talaat, M. Ipatov, J.M. Blanco, and V. Zhukova, *J. Alloys Compd.* 615, 610 (2014).
14. V. Zhukova, M. Ipatov, A. Talaat, J.M. Blanco, M. Churyukanova, and A. Zhukov, *J. Alloys Compd.* 707, 189 (2017).
15. H. Chiriac, T. Ovari, and Gh. Pop, *Phys. Rev. B* 52, 10104 (1995).
16. M. Vazquez and A. Hernando, *J. Phys. D Appl. Phys.* 29, 939 (1996).
17. M. Vazquez and A.P. Zhukov, *J. Magn. Magn. Mater.* 160, 223 (1996).
18. M. Vázquez, *Phys. B* 299, 302 (2001).
19. A.S. Antonov, V.T. Borisov, O.V. Borisov, A.F. Prokoshin, and N.A. Usov, *J. Phys. D Appl. Phys.* 33, 1161 (2000).
20. G.R. Aranda, N.A. Usov, V. Zhukova, A. Zhukov, and J. Gonzalez, *Phys. Status Solidi A* 205, 1800 (2008).
21. A. Zhukov, A. Talaat, M. Ipatov, and V. Zhukova, *IEEE Magn. Lett.* 6, 2500104 (2015).
22. A. Zhukov, M. Ipatov, M. Churyukanova, S. Kaloshkin, and V. Zhukova, *J. Alloys Compd.* 586, S279 (2014).
23. A. Zhukov, M. Ipatov, M. Churyukanova, A. Talaat, J.M. Blanco, and V. Zhukova, *J. Alloys Compd.* 727, 887 (2017).
24. C.F. Catalan, V.M. Prida, J. Alonso, M. Vázquez, A. Zhukov, B. Hernando, and J. Velázquez, *Mater. Sci. Eng. A, Supplement*, 438–441 (1997).
25. H. Chiriac, T.A. Ovari, Gh. Pop, and F. Barariu, *IEEE Trans. Magn.* 33, 782 (1997).
26. M.J. Garcia Prieto, E. Pina, A. Zhukov, V. Larin, P. Marin, M. Vazquez, and A. Hernando, *Sens. Actuators A* 81, 227 (2000).
27. A. Zhukov, J.M. Blanco, J. González, M.J. Garcia Prieto, E. Pina, and M. Vázquez, *J. Appl. Phys.* 87, 1402 (2000).
28. S. Corodeanu, T.-A. Ovari, and H. Chiriac, *IEEE Trans. Magn.* 50, 2007204 (2014).
29. A. Zhukov, *Novel Functional Magnetic Materials* (Berlin: Springer, 2016).
30. V.A. Bautin, E.V. Kostitsyna, A.V. Popova, S.A. Gudoshnikov, A.S. Ignatov, and N.A. Usov, *J. Alloys Compd.* 731, 18 (2018).
31. A. Zhukov, V. Zhukova, J.M. Blanco, A.F. Cobeno, M. Vazquez, and J. Gonzalez, *J. Magn. Magn. Mater.* 258–259, 151 (2003).
32. S. Gudoshnikov, M. Churyukanova, S. Kaloshkin, A. Zhukov, V. Zhukova, and N.A. Usov, *J. Magn. Magn. Mater.* 387, 53 (2015).
33. E. Kostitsyna, S. Gudoshnikov, A. Popova, M. Petrzhik, V.P. Tarasov, N.A. Usov, and A.S. Ignatov, *J. Alloys Compd.* 707, 199 (2017).
34. H. Miwa, *Glass etching composition and method for frosting using the same*, US patent 6807824 B1.
35. R.D. Hardy and J.E. Jarufe, *Method and composition for etching glass ceramic and porcelain surfaces*, US patent 6337029 B1.
36. N.A. Usov, A.S. Antonov, and A.N. Lagar'kov, *J. Magn. Magn. Mater.* 185, 159 (1998).
37. N.A. Usov and S.A. Gudoshnikov, *J. Appl. Phys.* 113, 243902 (2013).
38. H. Bateman and A. Erdelyi, *Higher Transcendental Functions*, Vol. 2 (New York: McGraw-Hill Book, 1953).

**Publisher's Note** Springer Nature remains neutral with regard to jurisdictional claims in published maps and institutional affiliations.